

Effect of Residual Oil Saturation and Salinity on HPAM Rheology in Porous Media

R.S. Seright^{1*}, Madhar Sahib Azad², Mohammad B. Abdullah^{3,4}, and Mojdeh Delshad³

¹New Mexico Institute of Mining & Technology, Socorro, NM, USA

² King Fahd University of Petroleum & Minerals, Dhahran, Saudi Arabia

³ University of Texas at Austin, Austin, TX, USA

⁴ Kuwait University, Kuwait

*Corresponding author

Abstract

During polymer flooding, the velocities where shear-thickening occurs directly impact HPAM injectivity, fracture initiation, and whether viscoelasticity is significant in oil recovery. The onset velocity for shear-thickening in oil-free porous media is known to translate with the square root of permeability-porosity. However, few studies report HPAM rheology with residual oil present, and those conflict and are inconsistent with behavior seen without oil. This paper experimentally clarifies how S_{or} , salinity, and temperature impact HPAM rheology in rock.

HPAM rheology at 20°C was determined in Berea sandstone for Darcy velocities from 0.01 to 100 ft/d, S_{or} from zero to 0.55, and k_{rw} from 0.03 to 1. In a given experiment, the core was first exposed to the highest pressure-gradient for the test series. After stabilization, resistance factors were recorded and effluent viscosity was measured. Next, the velocity was halved, and the stabilization and measurement processes were repeated. This procedure was extended in steps to the lowest velocities. We also studied the effect of salinity on HPAM rheology in porous media between 0.105% to 10.5% TDS for 0.1% and 0.2% HPAM (at 20°C). Temperature effects on rheology in Berea from 20°C to 60°C were investigated using 0.2% HPAM in 0.105%-TDS water.

This work provides key information that will be crucial to establishing whether HPAM viscoelasticity can play a significant role in recovering oil in field polymer floods. It also provides crucial information for analytical/numerical efforts to establish when fractures will initiate and how far they will extend from the wellbore during polymer flooding field applications.

Introduction/Literature Review

HPAM Rheology in Porous Media.

When projecting the performance of a polymer flood, modelers/simulators often require input of rheological properties of polymer solutions in porous media under conditions relevant to the reservoir of interest. Over the range of velocities that might be encountered in a field application, synthetic polymers (notably HPAM or partially hydrolyzed polyacrylamide) usually exhibit the behavior shown in Figure 1 (adapted from Seright et al. 2011). In this figure, resistance factor is defined as brine mobility divided by polymer mobility in a given porous medium. Resistance factor may often be thought of as the effective viscosity of the polymer solution (relative to water) in porous media. Of course, solution viscosity and resistance factor increase with increased polymer concentration. At very low velocities (depending on polymer Mw, concentration and composition and rock permeability and lithology), Newtonian behavior may be seen (Seright et al. 2011). If the polymer concentration is low, a Newtonian regime is expected until a relatively high velocity is reached (Figure 1; Figure 4 of Chauveteau and Moan 1981; Figure 14 of Seright 2017). Also, Newtonian behavior may be seen to relatively high velocities if the rock is highly permeable (Cannella et al. 1988).

Shear thinning may occur as rate increases (0.2 to 10 ft/d in Figure 1). This rheology mimics that noted in a couette viscometer at low-moderate shear rates (black curve in Figure 2). The lower the permeability, the lower the velocity at which onset of the shear thinning occurs (Cannella et al. 1988). Shear thinning may not be seen when the polymer concentration is low. In Figure 1, shear thinning is only noted above 480-ppm HPAM, which is above the critical overlap concentration of 200 ppm.

As the velocity is increased further (above 10 ft/d in Figure 1), resistance factor increases with increased rate. In the petroleum literature, this behavior has commonly been called “shear-thickening”, although others have labeled it “dilatant”, “pseudo-dilatant”, “rheo-thickening”, “extensional-thickening”, “flow-thickening”, “porous-media thickening”, “elastic turbulence”, or “viscoelastic” (Chauveteau and Moan 1981; Durst et al. 1982; Heemskerk et al. 1984; Masuda et al. 1992; Seright et al. 2011; Howe et al. 2015; Jouenne and Heurteux 2020; Azad 2023). Shear thickening was noted in Figure 1 for all HPAM concentrations ranging from 25 ppm to 2500 ppm. This conveys that shear thickening is evident for both dilute and concentrated HPAM systems whereas shear thinning is evident only for concentrated systems. The hardening/thickening index quantifies the ability of the polymer to stretch and thicken (i.e.,

show an increase in viscosity with respect to strain rate). If the thickening is observed in a pure-extensional field, it is called strain hardening because the extensional field is a shear-free field and the polymer chain undergoes straining deformation and not shearing. If the thickening occurs in a shear field, it is called shear thickening because the thickening occurs without an extensional field (Azad 2023). Porous media thickening index quantifies the ability of the polymer chain to thicken in the presence of both shear and extensional fields.

At very high velocities (not illustrated in Figure 1), synthetic polymer molecules experience permanent breakage (commonly labelled “mechanical degradation”)—resulting in resistance factors appearing to decrease with increased rate (Seright et al. 1981; Seright and Wang 2023a). During polymer flooding, the velocities where shear-thickening occurs directly impact HPAM injectivity, fracture initiation, and whether viscoelasticity is significant in oil recovery of capillary-trapped residual oil with or without the presence of fractures (Seright 1983; Seright et al. 2009; Khodaverdian et al. 2010; Ma and McClure 2017; Azad et al. 2020a,b; Rock et al. 2020; Hwang et al. 2022; Sagyndikov et al. 2022; Abdullah et al. 2023; Li et al. 2023).

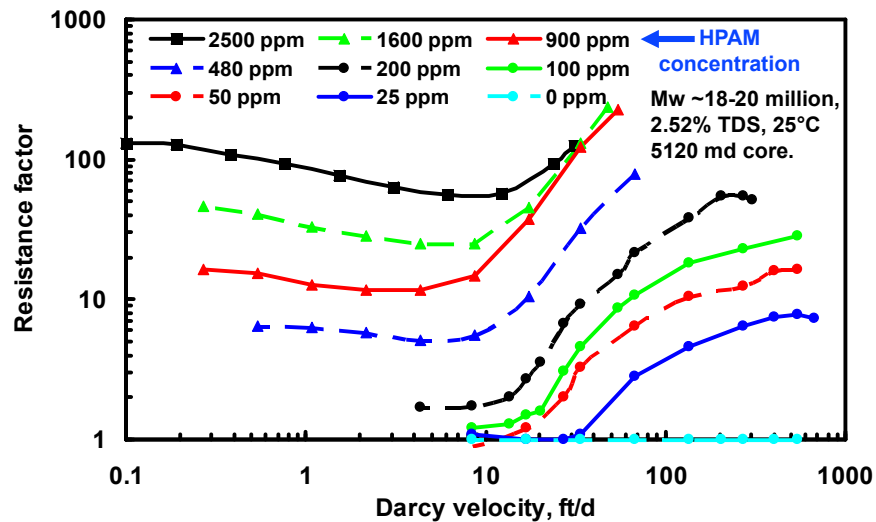


Figure 1—Effect of Darcy velocity and Flopaam 3830S HPAM concentration on rheology in porous polyethylene.

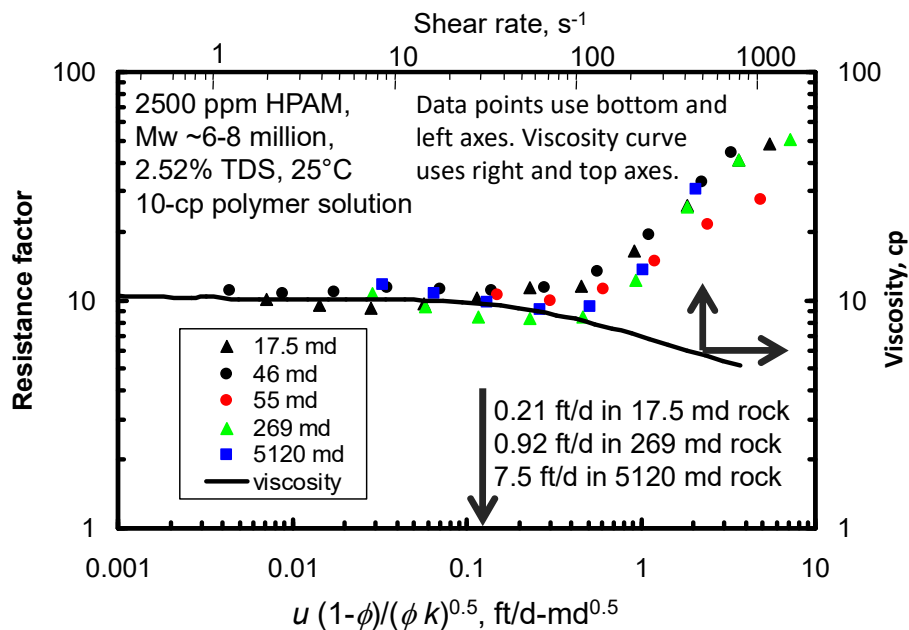


Figure 2—Resistance factor versus viscosity comparison (adapted from Seright et al. 2011).

Because the available studies of polymer rheology in porous media are limited, they do not cover the diverse range of salinity, hardness, temperature, oil saturation, and polymer concentration, Mw, or composition utilized in polymer flooding field applications. Consequently, models and simulators have relied heavily on assumptions and findings from rheological studies—since studies using a rheometer/viscometer are much easier and more convenient to perform than corefloods. However, that introduces uncertainty about

whether these rheology-based measurements are valid in porous media. This paper provides actual measurements of polymer rheology in porous media under different conditions of salinity (at a fixed ratio of NaCl/CaCl₂), HPAM concentration, oil saturation, and temperature, in hopes of improving assumed inputs for rheology parameters during simulations.

If no oil is present, polymer rheology in porous media correlates well with the parameters, $u/(k\phi)^{0.5}$ or $u(1-\phi)/(k\phi)^{0.5}$, where u is Darcy or superficial velocity, ϕ is porosity, and k is permeability (Cannella et al. 1988; Seright et al. 2011). This finding (demonstrated in Figure 2) has considerably simplified the job of modelers when attempting to account for permeability-porosity variations in a reservoir during simulations of chemical flooding. Many models and simulators (Hirasaki and Pope 1974; Chauveteau and Moen 1981; Cannella et al. 1988; Willhite and Uhl 1988; Seright 1991; Masuda et al. 1992; Delshad 2008; Lohne et al. 2017; Zeynalli et al. 2022) have attempted to convert velocities in porous media to an effective “shear rate” that is hoped will be directly relatable to shear rate in a viscometer. Although most of those models have the $u(1-\phi)/(k\phi)^{0.5}$ or $u/(k\phi)^{0.5}$ factor in common, they may assume different multipliers for this factor (e.g., 0.98 to 6 from Table II of Cannella et al. 1988).

Defining the Onset of Shear Thickening.

There are multiple ways that the onset of shear thickening in porous media can be defined. To understand the differences, consider Figure 3, which plots the resistance factor (on the y -axis) versus Darcy velocity (on the x -axis). Depending on the method used to define the onset of shear thickening, this figure may also attempt to superimpose a plot of viscosity versus shear rate. To accomplish this, the viscosity may need to be multiplied by a “ y -shift factor” and the shear rate may need to be multiplied by a “ x -shift factor”—as indicated in Figure 3. One method to define the onset of shear thickening (advocated by Chauveteau and Moan 1981) first finds a desired match/overlap between the viscosity-versus-shear-rate curve and the resistance factor-versus-velocity curve. Then select the point at which the resistance factor-versus-velocity curve (black curve in Figure 3) first departs from the viscosity-versus-shear-rate curve (green dashed curve in Figure 3.) That point is indicated by the red arrow in Figure 3. One can argue that above this velocity, any level of resistance factor that is above that expected from viscosity is due to viscoelastic effects. Several points of uncertainty surround this selection. First, as indicated in the previous paragraph, there is no universal agreement about the correct multiplier for conversion of velocities in porous media to shear rate in a viscometer. Consequently, the uncertainty in the x -axis shift factor will affect how the viscosity-versus-shear-rate curve is made to line up with the resistance-factor-versus-velocity curve. Second, (contrary to Figure 2) the zero-shear-rate viscosity may be different (usually lower) than the zero-velocity resistance factor (i.e., at the lowest rates in Figure 3). As a result, uncertainty is introduced on how to properly shift the viscosity data vertically to achieve alignment with the resistance-factor data. Some (e.g., Lohne et al. 2017) advocate that this vertical shift can be made by defining the apparent viscosity in porous media as water viscosity times the resistance factor divided by the residual resistance factor. (Residual resistance factor is defined as water mobility before exposure to polymer divided by water mobility after polymer is flushed from the core. It may be thought of as the permeability reduction caused by the polymer.) A major problem with that approach is that residual resistance factors are notoriously unreliable because of the way they are usually measured (Seright 2017; Wang et al. 2020; Seright and Wang 2023b). When water is injected to displace polymer, viscous fingers form so that a large volume of water is needed to properly displace the viscous polymer solution—often 100 pore volumes (PV) or more of water flush. Unfortunately, inconsistent and insufficient water flush volumes have been commonly used in the past, so reported residual resistance factors are frequently inconsistent and unrealistically high. These errors add to the uncertainty of the first method of assessing the onset of shear thickening.

A second method (Green and Willhite 2018) utilizes the intersection point of two extrapolated lines, indicated by the green arrow in Figure 3. The blue dashed curve in Figure 3 attempts to extrapolate the most linear part of the shear-thickening region of the resistance-factor curve. Where this extrapolation intersects the green-dashed viscosity curve is taken as the onset of shear thickening. This point can also be identified by plots of the log of pressure gradient versus velocity—where an extrapolation from the shear-thinning behavior intersects that from the shear-thickening behavior (Figure 7 of Heemskerk et al. 1984). This method suffers uncertainty in the proper choice of the most linear part of the shear-thickening region of the resistance-factor curve. (Not all the data points after the onset of shear thickening will always fit a linear trend.) It also suffers uncertainty from many of the factors mentioned above for the correct placement of the viscosity curve—unless the extrapolations are only performed using the resistance-factor-versus-velocity curve (i.e., completely ignoring the viscosity-versus-shear-rate curve).

A third method is to select the minimum in the resistance-factor-versus-velocity curve—indicated by the black arrow in Figure 3. The main uncertainty here is simply the proper selection of the minimum. This method avoids most of the uncertainties mentioned for the other two methods. Considering the experimental difficulties in using the first two methods, there may be high value in theoreticians relating their models to the resistance-factor minimum indicated in Figure 3. Note in the third method that a conversion to shear rate is not necessary—thus avoiding the uncertainties associated with the conversions from shear rates to velocities. Perhaps, other modeling efforts might benefit from a greater emphasis on utilizing velocities instead of “shear rates”.

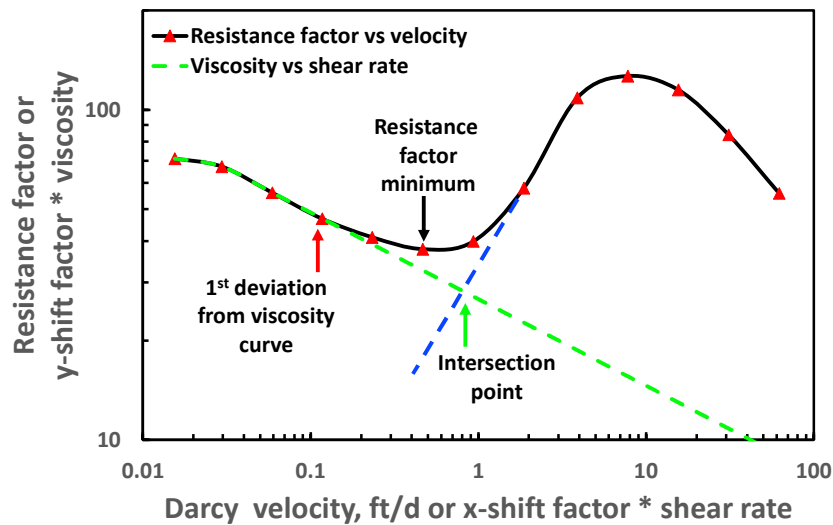


Figure 3—Alternative ways to define the onset of shear thickening in porous media.

Examination of Figure 3 reveals that the three different definitions can give greatly different onset velocities for shear thickening. Although the first definition has often been related to theoretical models, our experimental assessment will focus on the third method because it is the easiest to determine experimentally and because it involves the least uncertainty of the various methods.

Effect of Oil Saturation on Rheology in Porous Media.

Interestingly, while the $u(1-\phi)/(k\phi)^{0.5}$ or $u/(k\phi)^{0.5}$ shift factors have been shown to be valid in porous media without residual oil (i.e., Figure 2), it has limited validation when oil is present. When accounting for the presence of residual oil, porosity (ϕ) in the shift factor is replaced by the aqueous phase porosity [i.e., $\phi(1-S_{or})$, where S_{or} is residual oil saturation] and absolute permeability (k) is replaced by the effective permeability to water (k_w). With shear-thinning xanthan solutions in Berea sandstone, Figure 6 of Cannella et al. (1988) noted cases where the shift factor worked well with oil saturations of 0, 0.198, and 0.288. In contrast, the data of others (e.g., Figure 10 of Gumpenberger et al. 2012 and Figure 6 of Skauge et al. 2018) imply that HPAM rheology in porous media may not correlate well with the above shift factors if residual oil is present. Similarly, Alfazazi et al. (2021) found that an ATBS-acrylamide copolymer at 50°C in Indiana limestone showed an unexpected rheology shift with versus without residual oil present. Also, Masalmeh et al. (2019) found that an ATBS polymer at 50°C in reservoir carbonate cores showed an unexpected rheology shift with versus without residual oil. If correct, these suggestions would dramatically complicate predictions of the effects of rheology on polymer flooding in reservoirs. Consequently, one goal of this paper is to test the validity of the $u(1-\phi)/(k\phi)^{0.5}$ shift factor, as a function of oil saturation.

Effect of Polymer Mw, Polymer Concentration on Rheology in Porous Media. Not surprisingly, there is general agreement that the maximum resistance factor associated with shear thickening increases with increased HPAM molecular weight (Mw) and concentration. Also, general agreement exists that the onset velocity of shear thickening or the “polymer relaxation time” in porous media decreases with increased polymer Mw and decreased rock permeability (Jennings et al. 1971; Durst et al. 1982; Heemskerk et al. 1984; Howe et al. 2015). Concerning the effect of polymer concentration, Heemskerk et al. (1984) speculated the onset velocity should decrease with increased polymer concentration. In a series of short capillary expansions and contractions, Chauveteau and Moan (1981) noted the “wall shear rate” for onset of shear thickening decreased by a factor of five as HPAM concentration increased from 21 to 1360 ppm. However, in porous media, Jennings et al. (1971), Seright et al. (2011), and Howe et al. (2015) demonstrated that the decrease in velocity for the onset of shear thickening was quite modest with increased concentration (for 18-20 million g/mol Mw HPAM), especially for concentrations between 480 and 2500 ppm (see Figure 1).

Comparing the work of Seright et al. (2011) and Howe et al. (2015) with that Chauveteau and Moan (1981), the onset rate decreases considerably with respect to concentration in the case of Chauveteau and Moan’s work. Seright et al. (2011) measured the in-situ rheology in 5120-md porous polyethylene. Howe et al. (2015) measured the in-situ rheology in 3100-md homogeneous rock. Two interpretations can be made—first by considering the flow field alone, and second by considering the polymer-nature. The higher the permeability, homogeneity, or unconsolidated nature, the later the viscoelastic onset because polymer solutions will be less likely to experience substantial elongation. However, Chauveteau and Moan (1981) performed their in-situ rheology in a 3-D model characterized by a series of sharp expansion and contractions, which would give rise to a sharp and repeated elongation flow path.

A careful examination of Figure 3 of Howe et al. (2015) conveys that in steady shear rheometry, the onset rate remains the same for a concentration range of 0.03% to 0.24% for Flopaam 3630 HPAM. A careful examination of Figure 9 of Azad et al. (2018) shows that 0.2% Flopaam 3630 HPAM leads to an early onset rate of strain hardening in a pure extensional field when compared to 0.1% of this polymer. A stronger extensional flow field might have resulted in the decrease of onset rate with respect to increased HPAM concentration in the case of Chauveteau and Moan (1981).

Further, a careful look at Figure 8 of Seright et al. (2011) shows that a decreasing onset is evident with increasing concentrations when the HPAM concentration is below 200 ppm. In contrast, in Figure 4 of Chauveteau and Moan (1981), a decreasing onset with increasing concentration is seen even up to 1300 ppm polymer. A possibility for this discrepancy is that in Chauveteau’s work, a relatively low Mw of polymer (7 million g/mol) was used, whereas in the work of Seright et al. (2011) and Howe et al. (2015), ~19-million-g/mol-Mw polymer was used. Perhaps, low-Mw polymer may have a higher critical overlap concentration and an earlier onset of thickening for high polymer concentrations.

Effect of Salinity and Temperature on Rheology in Porous Media.

Heemskerk et al. (1984) speculated the velocity for the onset of shear thickening should increase with increased salinity and temperature. However, no supporting evidence was provided. A notable number of studies of synthetic-polymer rheology in porous media have been conducted using a wide range of conditions (e.g., Hirasaki and Pope 1974; Seright 1983,2009,2011,2021; Masuda et al. 1992; Howe et al. 2015; Lohne et al. 2017; Masalmeh et al. 2019; Alfazazi et al. 2021; Zeynalli et al. 2023). Delshad et al. (2008); Lohne et al. (2017); Azad and Trivedi (2019); and Zeynalli et al. (2023) formulated models/equations that were used to characterize many published data sets for rheology in porous media. However, the diverse combination of polymer Mw, concentration, source, salinity, temperature, and core material do not allow definitive conclusions to be made on the effects of salinity or temperature on the onset of shear thickening. Consequently, another goal of this work is to examine the effect of salinity and temperature on the onset velocity under controlled conditions.

In a viscometer while testing polyacrylamide/water glycerol solutions, Briscoe et al. (1999) noted that the shear rate for onset of shear thickening roughly doubled as temperature increased from 17° to 35°C. However, increasing the salinity from 2% to 5.85% NaCl had no discernable effect on the shear rate for onset of shear thickening. Azad (2023) reported that varying the salinity from 0.5% to 2% did not affect the onset of shear thickening for 0.1% Flopaam 3630 HPAM. Lohne et al. (2017) and Skauge et al. (2018) suggested that temperature may increase the velocity for onset of shear thickening in two ways. First, water viscosity decreases with increased temperature following an Arrhenius relation $[e^{-x/(RT)}]$. Second, as temperature increases, solvent quality decreases, resulting in more compact polymer coils and possibly longer velocities for onset of shear thickening. Experimental verification is needed to test these concepts.

Consequently, this paper will provide experimental clarification for how oil saturation, salinity, and temperature affect shear thickening behavior for HPAM solutions (in Berea sandstone).

Materials and Methods

Polymer, Solutions, and Oil.

All salt solutions in this work contained a NaCl/CaCl₂ ratio of 20:1 by weight. Seven salinities were examined as indicated in Table 1, with total salinities (total dissolved solids or TDS) ranging from 0.105% to 10.5%. The oil used for some experiments was Equate™ mineral oil (from Walmart), which had a viscosity of 210 cp at 20°C.

Table 1—Salinities used in this work.

Total salinity, %TDS	0.105	0.21	0.525	1.05	2.1	5.25	10.5
Wt. % of NaCl	0.1	0.2	0.5	1	2	5	10
Wt. % of CaCl ₂	0.005	0.01	0.025	0.05	0.1	0.25	0.5

The HPAM polymer used in this work was SNF Flopaam 3630S™, lot #GJ1201. The manufacturer indicated that this co-polymer contained ~70% acrylamide groups and ~30% acrylate groups and had a molecular weight of 18-20 million g/mol. Polymer solutions were prepared by sprinkling HPAM onto the shoulder of a vortex created using IKA20 overhead stirrers. Solutions were stirred overnight.

Polymer solution viscosities were measured using a Vilastic V-E rheometer. Figures 4 and 5 plot viscosity versus shear rate and salinity (at 20°C) for HPAM concentrations of 1000-ppm and 2000-ppm, respectively. As expected, viscosity decreased with increasing salinity and increased with increased polymer concentration. At low shear rates (<1 s⁻¹), viscosity was 10-14 times greater at 0.105% TDS than at 10.5% TDS, depending on polymer concentration. At low shear rates with 0.105% TDS, viscosity was 4.5 times greater with 2000-ppm HPAM than with 1000-ppm. At low shear rates with 10.5% TDS, viscosity was 3.3 times greater with 2000-ppm HPAM than with 1000-ppm HPAM.

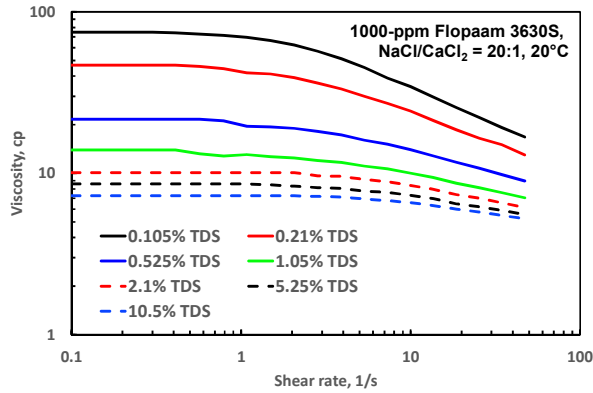


Figure 4—Viscosity vs shear rate and salinity for 1000-ppm HPAM.

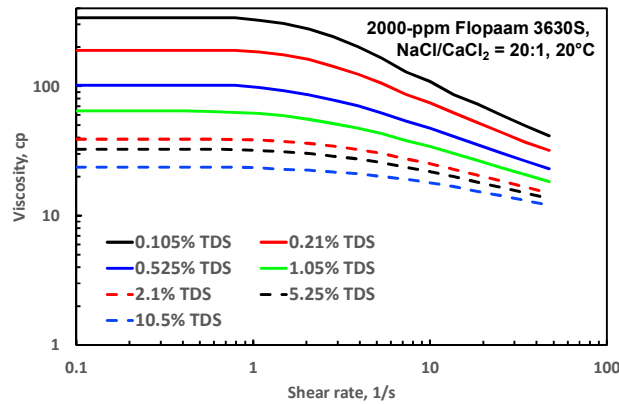


Figure 5—Viscosity vs shear rate and salinity for 2000-ppm HPAM.

Cores and Corefloods.

Berea sandstone cores were used in this work, with porosity of 0.21 and absolute permeability (to water) ranging from 204 to 252 md. Cores were 2.54-cm in diameter and either 15.24-cm or 30.48-cm in length, with an internal pressure tap located 7.62-cm from the inlet core face. Dry cores were placed within a CoreLab rubber sleeve and confined with 1500-psi pressure. A high vacuum was applied to the dry cores before saturating with brine and measuring permeability to water. For two of the cores (i.e., 210-md core for the work with different oil saturations and 252-md core with 2000-ppm HPAM), permeability was quite constant through the different sections of the cores. However, for the 204-md core used with 1000-ppm HPAM, the first 7.62-cm section had a permeability of 106 md, while the last 22.86-cm section had a permeability of 293-md.

Results and Discussion

Rheology in Porous Media Without Residual Oil.

To establish a baseline of behavior, a 1000-ppm HPAM solution in 1.05% TDS brine was injected into a 15.24-cm long, 210-md Berea core using a Darcy velocity (equivalent to flux or superficial velocity) of 59 ft/d (pressure gradient of 2600 psi/ft; volumetric rate of 6.33 cm³/min). After stabilization, pressures and flow rate were recorded and resistance factor was calculated. Next, the injection rate was halved and pressures and rates allowed to stabilize again. This process was repeated in steps to low rates (i.e., Darcy velocity of 0.0155 ft/d or volumetric rate of 0.00166 cm³/min). The dashed black curve in Figure 6 plots resistance factors from this procedure. After the lowest rates were achieved, rates were increased in stages back to the highest rate. The blue curve in Figure 6 shows those results and demonstrates that the behavior was reasonably reproducible. Previous work (Seright 1983, Seright et al. 2009, 2011) explained the various segments of the rheological curve. At the lowest rates, resistance factor behavior parallels rheology in a viscometer. Resistance factor and viscosity both exhibit Newtonian rheology at the lowest rates (Darcy velocity or shear rate, respectively). As rate was increased, shear thinning behavior was seen in both porous media and a viscometer (Figures 4 and 6), where resistance factor and viscosity both decrease with increased rate. At rates higher than 1 ft/d, shear thickening (or viscoelastic) behavior was exhibited in porous media, up to a maximum of 15 ft/d. At higher Darcy velocities, resistance factor appeared to decrease—due to progressively greater irreversible mechanical degradation of the polymer (i.e., breakage of polymer chains) with each higher rate.

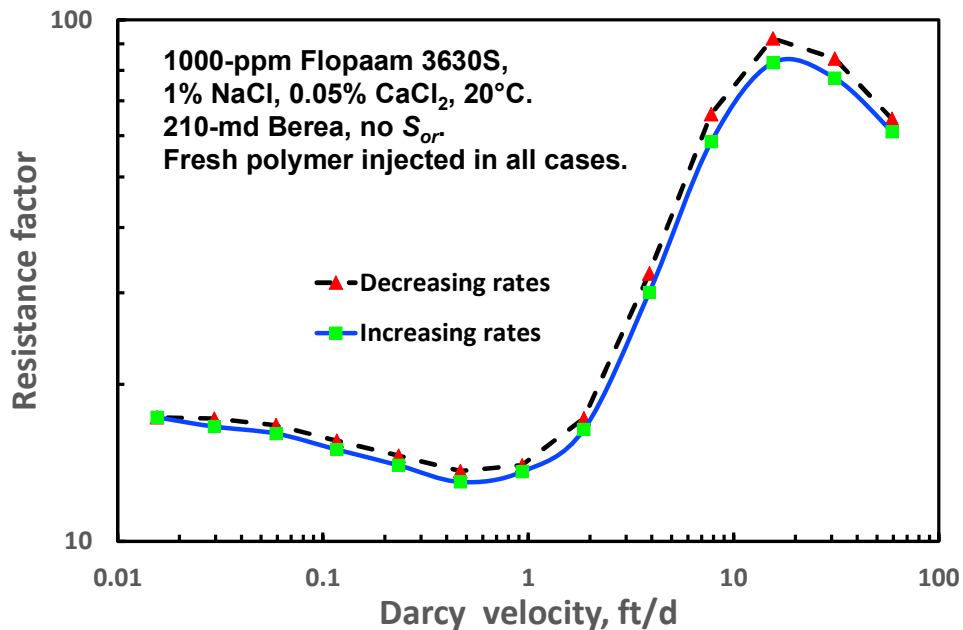


Figure 6—Rheology in porous media without residual oil.

Effect of Residual Oil Saturation (S_{or}) on HPAM Rheology in Porous Media.

Many examples exist in the literature where rheology in porous media was determined in the absence of residual oil. With no residual oil present, Seright et al. (2011) demonstrated that the rheology curves shift quite predictably with variations in permeability and porosity, using the factor: $u(1-\phi)/(k\phi)^{0.5}$. The presence of residual oil is known to dramatically reduce permeability to water, so one might expect this permeability-porosity shift factor to be applicable if residual oil was present and relative permeability to water was known. However, as mentioned in the literature review, data from several sources appears to contradict this expectation. For example, Figure 6 of Skauge et al. (2018) suggests that the velocity at which shear-thickening onsets and the range over which shear-thickening occurs are independent of oil saturation and wettability of the porous medium (for 500-ppm Flopaam 3630S in 1% NaCl brine). Figure 10 of Gumpenberger et al. (2012) suggests that adding a residual oil saturation might increase the velocity for onset of shear thickening (for 1000-ppm Flopaam 3630S in 2.2% TDS brine)—which is in contradiction to expectations from the $u(1-\phi)/(k\phi)^{0.5}$ or $u/(k\phi)^{0.5}$ shift factors. Since Skauge et al. (2018) or Gumpenberger et al. (2018) did not address these discrepancies in their papers, it may be possible that the discrepancies were simply due to experimental limitations of their data. Another unanswered question is whether oil viscosity impacts the onset of shear thickening.

To pin down how a resident oil saturation impacts HPAM rheology, further experiments were performed following that associated with Figure 6. HPAM rheology was determined for five levels of oil saturation, as indicated in Table 2. Case 1 is that associated with Figure 6, where no oil was present (so $S_{or}=0$). In Cases 2-5, six pore volumes (100 cm³) of 210-cp mineral oil (Equate™ brand at 20°C) were forced through the core using a pressure gradient of 2600 psi/ft to establish an irreducible or connate water saturation ($S_{wr}\sim 0.15$). For Case 2, 1000-ppm HPAM (in 1.05% TDS brine) was injected using a fixed pressure gradient of 2600 psi/ft to establish a residual oil saturation of about 0.1, corresponding to a capillary number of 3.8×10^{-4} . (Due to experimental error—associated with collecting a small oil volume with a large water volume at high rates, there may be significant error bars on the S_{or} measurements listed in Table 2—e.g., ± 0.03 saturation units. However, as will be demonstrated by comparing Figures 8 and 9, these potential S_{or} errors have a minor effect on shifting the rheological curves compared to k_{rw} values.) (We used the highest pressure gradients first in these experiments to minimize the impact of capillary desaturation during subsequent injections using lower pressure gradients. During either oil or polymer injection at the highest rate/pressure gradient, flow was controlled by constant pressure drop across the core. During subsequent, lower-rate injections, flow was controlled by constant injection rate. These steps were accomplished using ISCO 500D™ pumps.) After stabilization of pressure and flow rate, a resistance factor was calculated and recorded, and the injection rate was halved. This procedure was repeated to the lowest rates, as indicated by the solid red circles/red curve in Figure 7. No further production of oil was noted during this part of the experiment. Thus, the red rheological curve in Figure 7 was presumed to be conducted entirely with a fixed S_{or} of ~ 0.1 .

After achieving the lowest rate, mineral oil was again injected at 2600 psi/ft in an attempt to drive the core back to a consistent S_{wr} starting point (~ 0.15). Then, for Case 3, 1000-ppm HPAM was injected using a maximum pressure gradient of 1200 psi/ft to establish an S_{or} of ~ 0.2 . The injection rate was again reduced in steps to produce the blue curve in Figure 7. The entire procedure of this paragraph was repeated two more times, using maximum HPAM pressure gradients of 600 and 356 psi/ft to determine the black and green curves in Figure 7, for S_{or} values of ~ 0.3 and 0.55, respectively. The resistance factor measurements reported on the y-axis of Figure 7 all assumed the same brine mobility—where no oil was present before any polymer injection. This was done because the k_{rw} values (for Cases 2-5) were not known at the time of the experiments.

Table 2—Various cases with different S_{or} and k_{rw} values.

Case	Max polymer Δp , psi	Max dp/dl , psi/ft	Minimum resistance factor in Fig. 7	S_{or}	k_{rw}
1	No oil	2600	13.6	0	1
2	1300 psi	2600	27.8	0.1	0.49
3	600 psi	1200	47.0	0.2	0.29
4	300 psi	600	118.8	0.3	0.11
5	178 psi	356	453.5	0.55	0.03

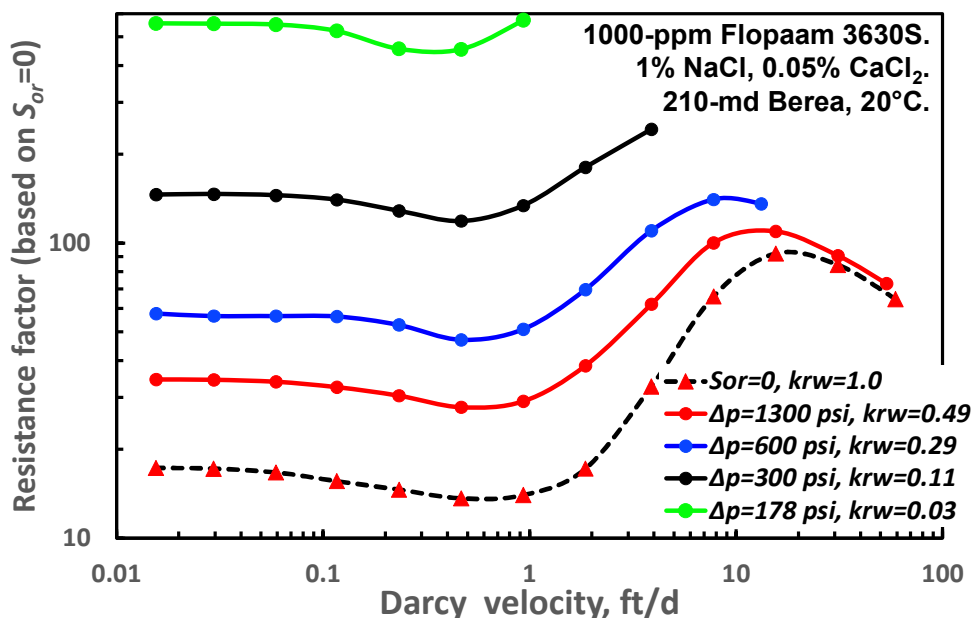


Figure 7—Rheology in porous media for various cases.

Note that a minimum resistance factor was observed for each of the five curves in Figure 7. We assumed that this minimum resistance factor reflects the k_{rw} value for the given oil saturation. Consequently, we estimated k_{rw} for Cases 2-5 by dividing the minimum resistance factor for Case 1 by the minimum resistance factor for a given case. The results of these calculations are listed in the last column of Table 2—yielding k_{rw} values of 1, 0.49, 0.29, 0.11, and 0.03, respectively. The resistance factors were then recalculated using these k_{rw} values and replotted in Figure 8 (i.e., the resistance factors from Figure 7 were multiplied by the corresponding k_{rw} value and then replotted in Figure 8).

On the x -axis of Figure 8, we multiply the Darcy velocity (u) from Figure 7 times the shift factor, $[1-\phi(1-S_{or})]/[k_{rw}\phi(1-S_{or})]^{0.5}$. As is evident, the standard permeability-porosity shift factor now works very well. This observation should bring considerable comfort to polymer flooding simulators who have assumed that this relation should hold during their many previous simulations of polymer flooding. The primary conditions where the relation does not appear to hold is at the higher rates—where the curves clearly diverge in behavior in Figure 8. The important implication of Figure 8 is that standard existing assumptions in simulators may predict polymer mobility fairly well at moderate to low rates—i.e., below 0.3 for the shift factor value associated with the x -axis in Figure 8. But they may break down if attempting to make predictions of injectivity and viscoelastic effects for higher velocities assumed with unfractured vertical polymer injection wells.

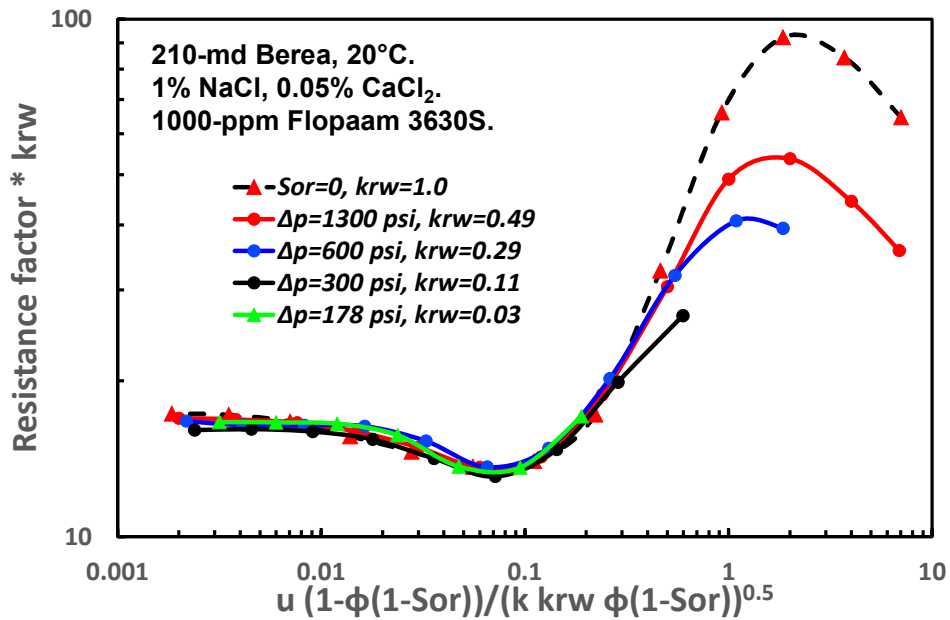


Figure 8—Correlating rheology incorporating S_{or} into aqueous phase porosity.

Figure 9 replots the same data from Figure 8, except the residual oil saturation was excluded from the x -axis. Excluding the oil saturation makes the effective aqueous-phase porosity somewhat higher. The match shown in Figure 9 was quite good, but not as good as that in Figure 8. Thus, (as mentioned in the parenthetical comment about S_{or} uncertainties in Table 2) excluding S_{or} from the porosity factor only makes a modest difference—so errors in S_{or} measurement are not particularly important. Measurements/values of k_{rw} are much more important.

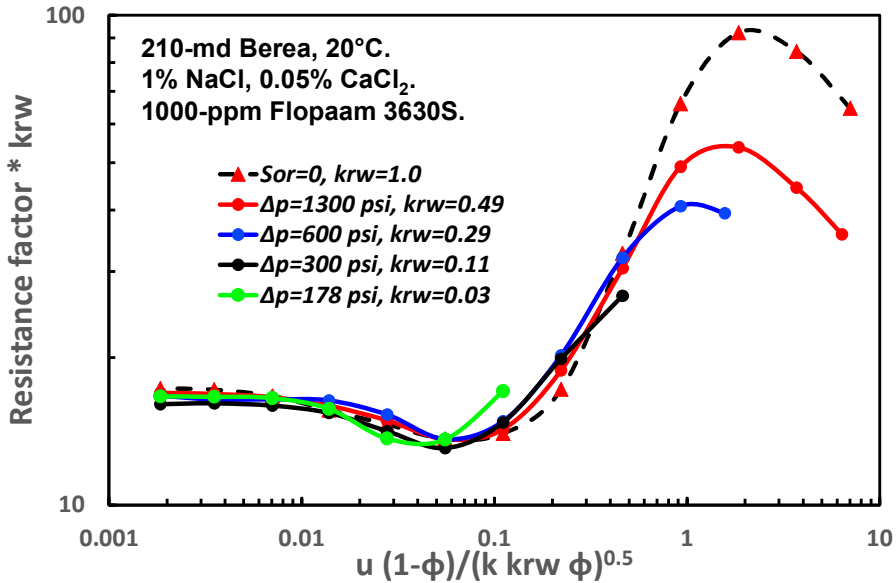


Figure 9—Correlating HPAM rheology without incorporating S_{or} into aqueous phase porosity.

For the final step of this part of the experiment, the core was again flushed with oil using 2600 psi/ft, and HPAM was again injected at 2600 psi/ft. Then the rheology curve was re-measured (blacked dashed curve in Figure 10) to see how closely it would match the solid red curve of Figure 7. The excellent match of the two curves in Figure 10 demonstrates that the rheology behavior for the first S_{or} case was the same as the last S_{or} case (i.e., the oil/polymer saturation process was reversible). If hysteresis had occurred during the various imbibition and drainage cycles, this result might not have occurred.

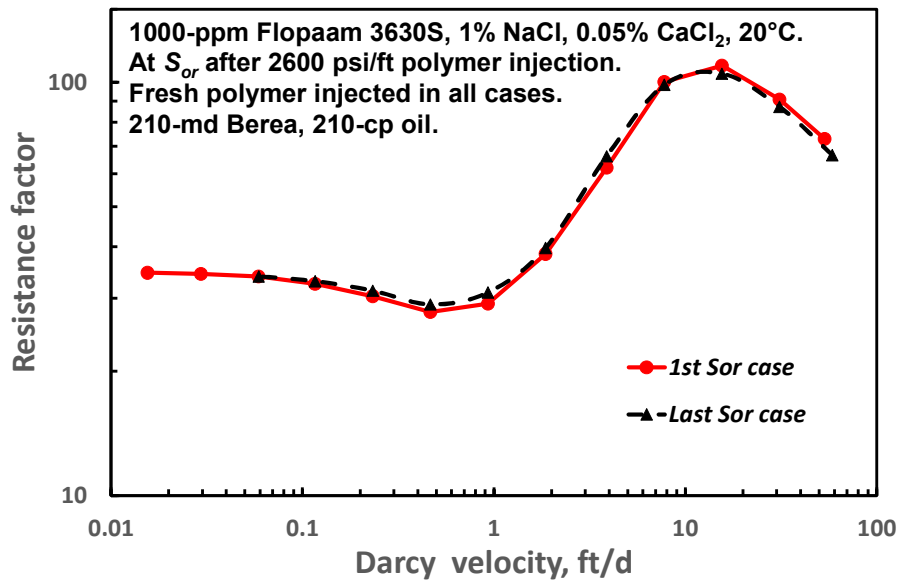


Figure 10—Reproducibility of rheology with oil present.

Apparent Contradictions from the Literature. Why did the data of others suggest that the $[I-\phi(1-S_{or})]/[k k_{rw} \phi(1-S_{or})]^{0.5}$ shift factor might not be valid? Let's examine individual literature reports, in search of an explanation. Figure 6 of Skauge et al. (2018) indicated that the onset of HPAM shear thickening (in Bentheimer sandstone) occurred at the same interstitial velocity, with $S_{or}=0.22$ versus without residual oil. In contrast, our comparisons were made using Darcy velocities. In Skauge's case, the interstitial velocity was 4-5 times greater than the Darcy velocity, but the interstitial velocity at S_{or} would only be about 20% faster than that without residual oil. Thus, the difference between interstitial and Darcy velocity cannot explain the results. Based on the $[I-\phi(1-S_{or})]/[k k_{rw} \phi(1-S_{or})]^{0.5}$ shift factor, one would expect the effective permeability to water should be much lower at S_{or} than with no oil present. For two cases reported by Skauge, the k_{rw} values were 0.12 and 0.2—leading to expected shift values of 0.34 and 0.45, respectively. In contrast, Figure 6 of Skauge et al. (2018) did not reveal any shift in the onset velocity for shear thickening. No explanation for the difference from our results is evident. Our 210-md Berea sandstone is expected to have a similar pore structure to their ~2-Darcy Bentheimer sandstone. Our 210-cp mineral oil should not behave radically differently from their 210-cp oil, and both experiments were performed at room temperature. Their experiments were performed with 500-ppm Flopaam 3630S, while ours used 1000 ppm. Their salinity was 0.4659% TDS, while ours was 1.05% TDS. Skauge et al. (2018) also reported that resistance factors in the presence of residual oil were substantially lower (e.g., by a factor of 3-4) than without oil. We did not see this effect at moderate to low velocities (see Figures 7 and 8 above). Possibly, this difference may be due to how the resistance factor was defined for their experiments—which is not clear to us. At any rate, if Skauge's results are accepted at face value, they would dramatically complicate how modelers input rheological parameters (and even polymer viscosity) into their simulators. In contrast, at moderate to low rates, our results would endorse previous assumptions made by modelers—that any shifts in polymer rheology are dominated by predictable shifts in effective permeability to water. Note that Figure 8 and Table 2 suggest that this statement is only valid for velocities below about three times the onset of shear thickening. Above that velocity, qualitatively consistent with Skauge's results, the resistance factors were moderated with increased S_{or} and decreased k_{rw} .

Alfazazi et al. (2021) studied shear thickening of 1000-ppm ATBS-acrylamide copolymer (8 million g/mol Mw) in 165-189-md Indiana limestone cores with versus without residual oil. They reported that the presence of residual oil actually increased the onset velocity for shear thickening—and like Skauge et al. (2018), observed that resistance factor at all velocities (both above and below the onset velocity) were substantially below those without oil. As noted in the previous paragraph, this behavior will considerably complicate the prediction of polymer behavior in field polymer floods—if the findings are proven valid.

In 2050-md Nordham sandstone, Gumpenberger et al. (2012) reported that 1000-ppm 3630S (in 2.2% TDS brine at 30°C) also found that residual oil did not decrease the onset velocity for shear thickening. However, contrary to Skauge et al. (2018) and Alfazazi et al. (2021), they reported that the presence of S_{or} substantially increased the resistance factor at all velocities.

In carbonate reservoir cores using 1000-ppm poly(ATBS) (i.e., SNF SAV10™), Masalmeh et al. (2019, Figure 15) noted that the onset velocity for shear thickening was not reduced by the presence of residual oil. Consistent with the literature above and also our work, the presence of a residual oil saturation substantially moderated the magnitude of shear thickening.

To summarize, the previous literature, coupled with our new findings, point out three areas that need further consideration. First, all experiments (including ours) indicated that the presence of a residual oil saturation substantially moderates the magnitude of the shear thickening behavior. Some (Skauge et al. 2018; Masalmeh et al. 2019) suggested that this behavior accounts for polymer injectivity in field applications being surprisingly high, relative to water. As will be argued in a later section, this idea is not sufficient to justify assuming that fractures are not open during polymer injection into vertical wells.

Second, reports conflict on whether the presence of residual oil reduces the resistance factor for velocities at or below the onset velocity for shear thickening. Perhaps, because of how we defined resistance factor in the presence of residual oil, our findings indicate

that the magnitude and rheology of resistance factors below the shear thickening onset are quite consistent with expectations associated with the permeability reduction caused by the presence of residual oil. In contrast, Skauge et al. (2018) and Alfazazi et al. (2021) reported that residual oil substantially reduced these resistance factors, while Gumpenberger et al. (2012) reported it substantially increased resistance factors. In many of these cases, it was not clear how resistance factor was defined when residual oil was present. It is possible that this conflict might be mitigated or removed if the same definition was used by all.

Third, our findings in Figure 8 indicate that the $[1-\phi(1-S_{or})]/[k k_{rw} \phi(1-S_{or})]^{0.5}$ shift factor works when correlating the velocity onset of shear thickening with the reduction of permeability associated with an S_{or} . (In other words, we predict that the reduced k_{rw} associated with the presence of residual oil will significantly reduce the onset velocity for shear thickening.) In contrast, data in the above literature reports suggest that addition of residual oil has little or no effect on the onset velocity for shear thickening. This point has important consequences on how shear thickening affects injectivity, fracture extension, and mobilization of capillary-trapped residual oil. We note that none of the above authors discussed this issue in their papers. So, it is possible that they felt that the unexpected lack of a shift in the velocity onset was simply due to limitations with their data quality.

Obviously, more work is needed to understand these apparent conflicts.

Effect of Salinity on HPAM Rheology in Porous Media.

Literature reports to date investigating HPAM rheology in porous media involved a variety of conditions, but few studies have focused specifically on the question of how HPAM rheology in porous media varies over a broad range of salinity. Examination of previous studies makes it difficult to clearly discern the impact of salinity. To help clarify this issue, we conducted experiments using a broad range of salinities, as indicated in Table 1. All experiments in this series were done at 20°C with 1000-ppm Flopaam 3630S. The ratio of NaCl/CaCl₂ was 20:1 in all cases. All floods were performed in the same Berea sandstone core, which was 30.48-cm long and 2.54-cm in diameter. A 1500-psi confining pressure was applied, permeability was 204 md, porosity was 0.21, and no oil saturation was present. An internal pressure tap was located 7.62-cm from the inlet core face. The experiment with the highest salinity (10.5% TDS) was done first, followed by progressively less-saline solutions. At a given salinity, the highest rates were applied first, followed by progressively lower rates. Several pore volumes (PV) of fluid were flushed for stabilization for each case (except at the lowest rates).

Figure 11 shows the effect of salinity on HPAM rheology in 204-md Berea. As expected, for a given Darcy velocity, resistance factor (measured/averaged across the entire core) decreased with increased salinity. When the salinity was very high, no shear thinning was evident—exhibiting a direct transition from Newtonian to shear thickening. Interestingly, over the entire salinity range (0.105% to 10.5% TDS), the Darcy velocity for the onset of shear thickening was not sensitive to salinity—occurring at ~0.47 ft/d. Similarly, over the entire salinity range, the velocity for the peak resistance factor occurred at ~7.8 ft/d. For 0.5% to 2% NaCl, Azad (2023) reported the onset for shear thickening during rheometric studies was not sensitive to salinity. However, above 2% NaCl, the onset-rate decreased with increased salinity.

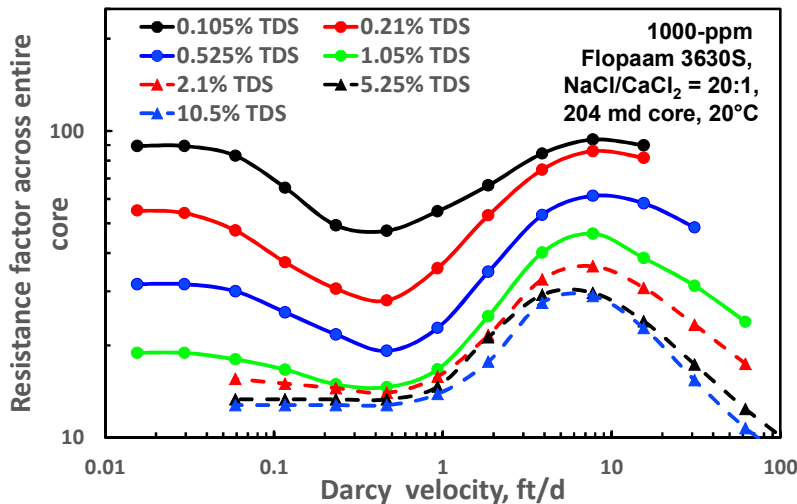


Figure 11—1000-ppm HPAM rheology based on measurements across the entire core.

Since an internal pressure tap was present, the resistance factor can also be calculated across the last three-quarters of the core. Those values are plotted for the various salinities in Figure 12, which qualitatively mimics Figure 11. Recall that the permeability of the second core section was 293 md, while the first core section (included in Figure 11) was 106 md.

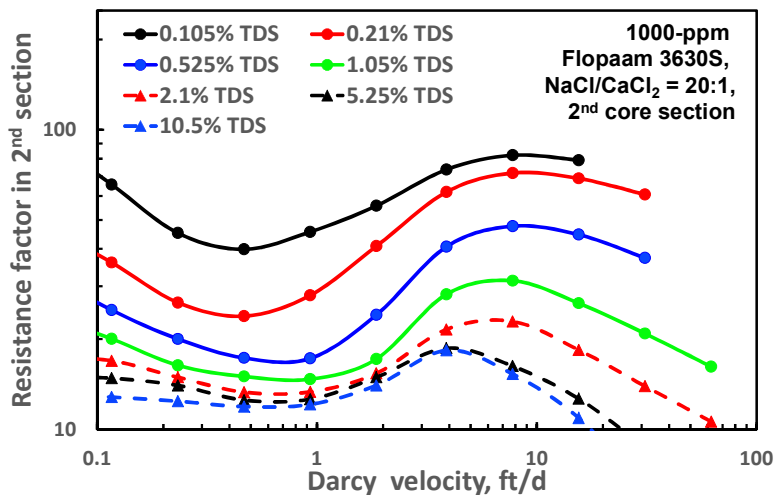


Figure 12—Rheology in second core section mimics the rheology across the entire core.

Seright (1983) noted that HPAM solutions can show an “entrance pressure drop” associated with polymer mechanical degradation at high velocities. Figure 13 illustrates the behavior reported by Seright (1983) for 500-ppm HPAM (Dow Pusher 700™) in 3.3% TDS brine in a 500-md Berea core. In this case, the pressure drop (and resistance factor) across the last three segments of the core were consistent, but the pressure drop across the first quarter of the core was notably greater than in the other segments. Seright (1983) proposed assigning “entrance pressure drop” to account for this behavior, and correlated the magnitude of the entrance pressure drop with the extent of mechanical degradation exhibited by the polymer. Seright (1983) demonstrated that this “entrance pressure drop” was not due to filtration of polymer or gel or a progressive plugging effect.

ENTRANCE PRESSURE DROP (SPE 9297)

- At high rates, high-Mw HPAM shows an excess pressure drop upon first entering a core.
- This entrance pressure drop is associated with HPAM mechanical degradation.
- The effect increases with increased rate.

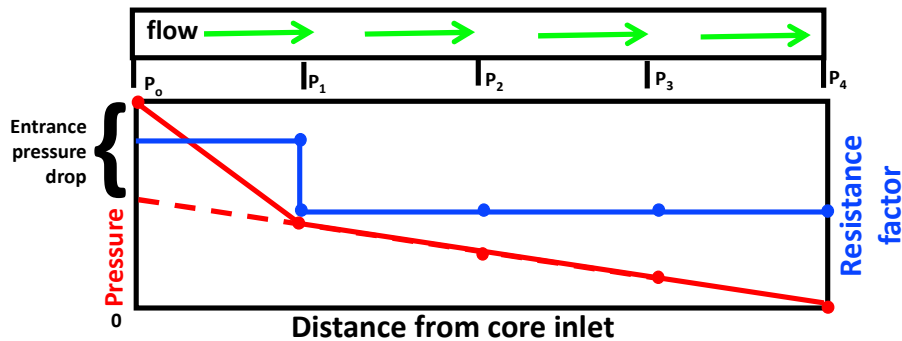


Figure 13—Illustration of the “entrance pressure drop” concept.

Figure 14 shows the entrance pressure drops calculated for our experiments with 1000-ppm HPAM and various salinities. Note that the entrance pressure drop was 0 below 1 ft/d, and increased with increased rate. The behavior was not sensitive to salinity.

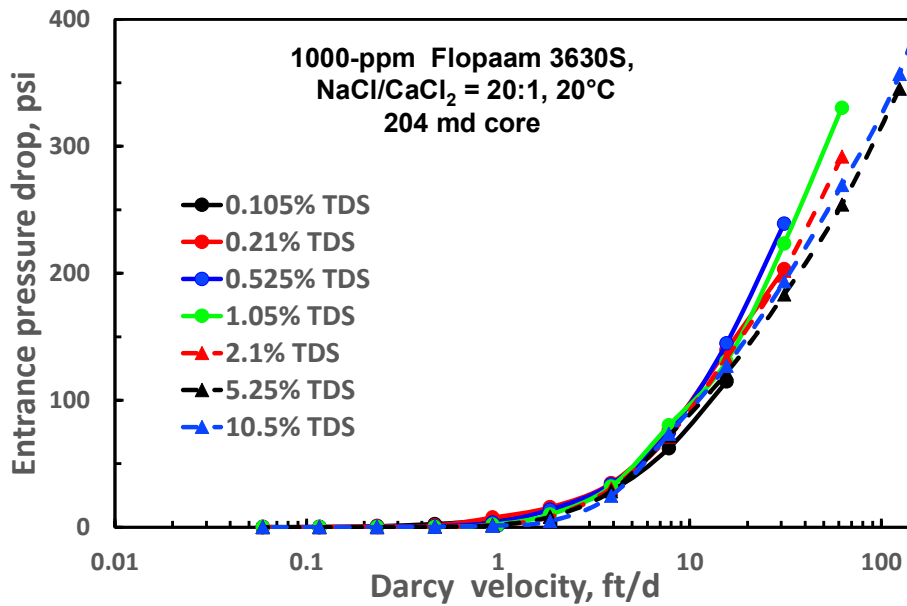


Figure 14—Entrance pressure drop versus rate and salinity for 1000-ppm HPAM.

Figure 15 shows that for a given velocity, shear degradation (as measured at 7.3 s^{-1} shear rate, 20°C) became more severe as salinity/hardness increased. The y-axis in Figures 15 and 17 is $100 \times [(\mu - \mu_s) / (\mu_o - \mu_s)]$ where μ_o is the original viscosity and μ_s is the solvent viscosity (i.e., 1 cp).

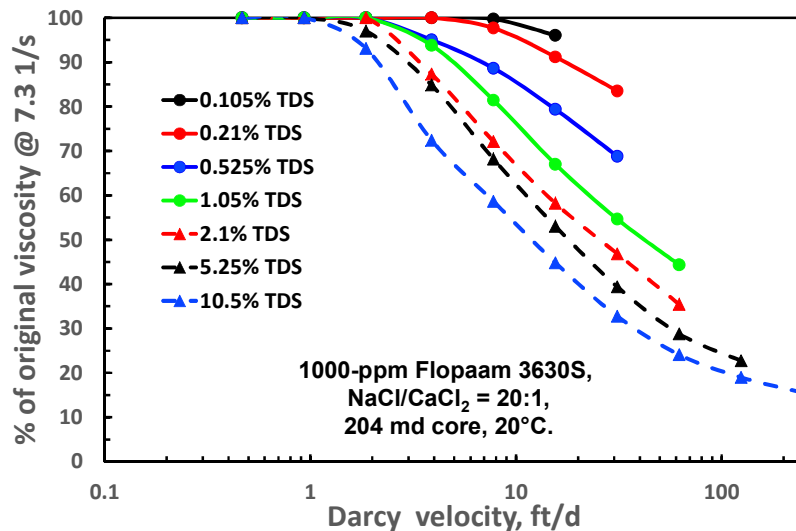


Figure 15—Mechanical degradation for 1000-ppm HPAM versus rate and salinity.

At very low salinity, the anionic carboxylate groups in HPAM molecules repel each other, thus expanding the polymer to a relatively large volume and allowing the polymer to provide a high viscosity. HPAM solution viscosity decreases dramatically with increased salinity, especially at low salinity. Increased ion concentrations screen HPAM's anionic carboxylate groups, reducing the polymer coil size, and decreasing solution shear viscosity. This salinity dependence may have been why Heemskerk et al. (1984) assumed that the onset of shear thickening should shift to higher rates as salinity increases. Zaitoun et al. (2012) convincingly argued that the tighter coils at higher salinities cause HPAM molecules to be less prone to untangle and elongate when forced through pore throats at higher rates—thus making them more susceptible to mechanical degradation as salinity increases. With this logic, one might expect that the polymer relaxation time, and therefore the onset of shear thickening, would be strongly affected by salinity. The fact that the onset is not sensitive to salinity should provide theoreticians more to consider. The onset of shear thickening may provide a measure of an onset of polymer solution's viscoelasticity—i.e., to transition from the shear-thinning regime to the shear thickening regime. The inverse of onset-rate gives a measure of a single relaxation time. For porous media applications, if the residential (observation) time experienced by the flowing polymer solutions is short enough relative to its relaxation time, they accumulate the un-relaxed stresses which eventually manifest in the form of additional viscosity (i.e., shear thickening phenomenon), more than expected from the simple shear viscosity. An important question includes, what level of viscosity increase is expected from shear thickening? Azad (2023) proposed that the

magnitude of the thickening can be quantified by fitting a power law to the shear thickening regime to calculate the shear thickening index (a strictly non-linear viscoelastic parameter that describes the slope of the viscosity increase in the shear thickening region). Though, we did not observe any change in the porous media thickening index with the wide range of salinity tested in this work (Figures 7 and 11) when a constant relaxation time was employed within the Unified Viscoelastic Model of Delshad et al. (2008). In contrast, Magbagbeola (2008) employed an oscillatory relaxation time which was higher for a low salinity polymer flood than a high salinity polymer flood; and therefore, resulted in a lower porous media strain hardening index for low salinity polymer systems (Table 5.3 of Magbagbeola 2008). Azad (2023) reported that despite having the same onset-rate, higher salinity polymer systems lead to higher shear thickening intensity. A variation in shear thickening index predicts a higher extent of mechanical degradation for high salinity polymer floods (Figure 21 of Azad 2023). Figure 15 of this paper confirms mechanical degradation to be higher for high salinity polymer floods than for less saline polymer floods. Jouenne and Huerteux (2020) stated “salinity does not impact the magnitude (of the shear thickening velocity region) except that the transition (to shear thickening as velocity is increased) is sharper as salinity increases.” The behavior shown in Figures 11 and 12 is more or less in agreement with that statement. Figure 9 of Jouenne and Huerteux (2020) suggest that the onset of shear thickening may occur at much lower velocity with 0.4%-NaCl than with 6% NaCl. However, these experiments were performed using different polymer concentrations, so it is not clear that they conflict with our results in Figures 11 and 12). However, Jouenne and Huerteux (2020) suggested that salinity has a minor effect on the degree of polymer degradation—which is not in agreement with Figure 15.

Effect of Polymer Concentration.

All of the experiments reported above were performed using 1000-ppm HPAM. This section will examine the rheology of 2000-ppm Flopaam 3630S versus rate and salinity. These experiments were conducted in a core, which was 15.24-cm long, 2.54-cm diameter Berea sandstone that had a permeability of 252 md, a porosity of 0.21, and no oil saturation. One internal pressure tap was located half way through the core. For 2000-ppm HPAM, Figures 16 and 17 plot results analogous to Figures 12 and 14. Comparing Figures 12 and 16 reveals that for both HPAM concentrations, the minimum in the resistance factor curves occurs around 0.47 ft/d, and the maximum of shear thickening curve occurs at ~7.8 ft/d. Thus, at both polymer concentrations, the velocity range for shear thickening was not sensitive to salinity, given a constant ratio of NaCl/CaCl₂. For cases with no oil present, this finding is consistent with previous reports (Seright et al. 2011; Howe et al. 2015; and Figure 1). This finding is also consistent with reported bulk shear rheological behavior where an increase in polymer concentration (between 0.03% to 0.24%) did not affect the onset-rate, even in a bulk shear field for Flopaam 3630 HPAM (Figure 3a of Howe et al. 2015). From linear oscillatory rheology, an increase in polymer concentration reportedly led to an increase in oscillatory relaxation time (Figure 3c of Howe et al. 2015). Steady shear rheometry may involve high shear rates, and therefore, may quantify non-linear viscoelastic effects. Several recent studies highlighted the importance of non-linear viscoelastic quantification for EOR applications (Howe et al. 2015; Jouenne and Heurteux 2020; Azad 2023).

Of course, we note the slightly exceptional curve for 2000-ppm HPAM in 10.5% TDS brine. At this very high salinity, the solvent-polymer interaction promotes a poor solvent quality—meaning that the polymer chains have a decreased preference to contact water, and the polymer may approach insolubility. (The solution was completely homogeneous and appeared totally dissolved, but it exhibited a significant Tyndall effect.) This effect might partially explain the delayed onset of shear thickening in 10.5% TDS brine.

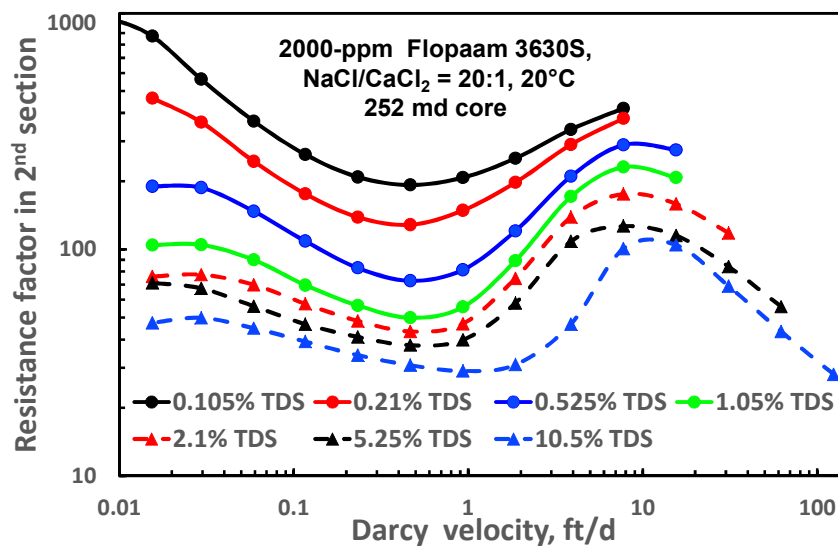


Figure 16—Resistance factor versus rate and salinity for 2000-ppm HPAM.

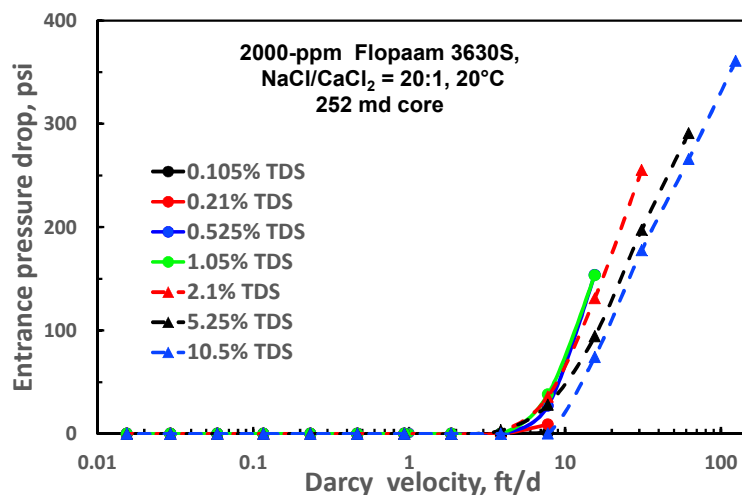


Figure 17—Entrance pressure drop versus rate and salinity for 2000-ppm HPAM.

Figure 18 compares the level of mechanical degradation for 2000-ppm HPAM versus for 1000-ppm HPAM. This comparison was made for a brine with 5% NaCl and 0.25% CaCl₂. For a given velocity, shear degradation was less with 2000-ppm HPAM than 1000-ppm HPAM. The core with 1000-md HPAM was notably less permeable (106 md in the first core section) than the core with 2000-md (252 md), and this fact could have influenced the degradation results. Note that mechanical degradation of polyacrylamides is only expected a high near-wellbore velocities. It is not expected to occur at moderate or low velocities (i.e., below 1 ft/d) deep within a reservoir (Seright 1983; Jouenne and Heurteux 2020).

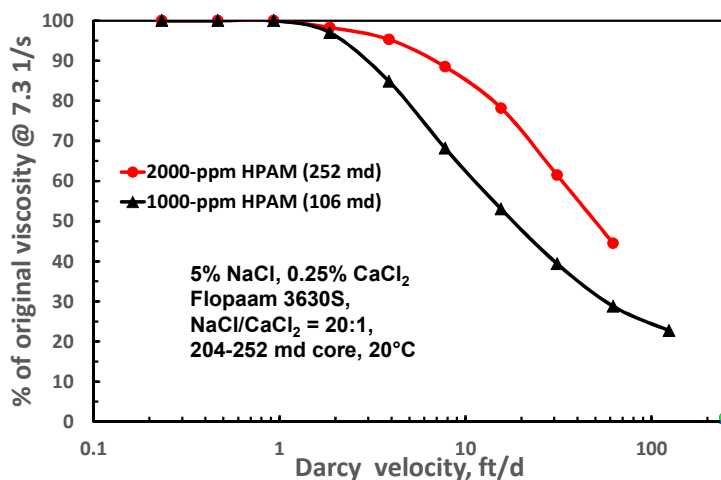


Figure 18—Mechanical degradation for 2000-ppm HPAM versus 1000-ppm HPAM.

Effect of Temperature on HPAM Rheology in Porous Media.

This section examines the effect of temperature (between 20°C and 60°C) for 2000-ppm Flopaam 3630S, 0.1% NaCl, 0.005% CaCl₂ in the 252-md core associated with the previous experiment. The experiments were performed in the same manner as those reported above (with no oil present). During this experiment, mechanical degradation was small/negligible for all rates up to 7.8 ft/d. No oxidative polymer degradation was noted at any rate during HPAM flow through the core at 20°C. Oxidative degradation was consistently about 3% at 40°C, independent of rate, and 7% at 60°C.

Figure 19 shows the effect of temperature on HPAM rheology in porous media. Resistance factors at each temperature have taken into account the reduction in brine viscosity with increased temperature. Water viscosity at 40°C was 0.652 times that at 20°C, and 60°C was 0.714 times that at 40°C. In Figure 19, the Darcy velocity associated with the minimum resistance factor at 40°C was roughly half that at 60°C and this minimum rate for 20°C was roughly half that at 40°C. Since our experiments involved consistently changing rates by a factor of two, it is conceivable that the shift factor could have been proportional to water viscosity (i.e., a factor of ~0.7 for each 20°C change in temperature). Examination of Figure 19 also reveals that the minimum in resistance factor at 40°C was 0.743 times that at 20°C, and the minimum in resistance factor at 60°C was 0.706 times that at 40°C. Thus, both the minimum resistance factor and the corresponding velocity associated with that minimum could be shifted by the same factor as the shift in water viscosity with temperature. The observed shift of the curves with Darcy velocity (as temperature increases) makes sense. However, since the resistance factors in Figure 19 already have accounted for the water viscosity shift with temperature, the behavior implies that the water viscosity squared

must somehow be incorporated into the resistance factor calculations to properly account for the observed behavior. Recall that oxidative and mechanical degradation was small throughout the experiments. Perhaps, as suggested by Lohne et al. (2017) and Skauge et al. (2018), the additional shift in onset to higher velocities is due to reduced solvent quality and HPAM coil shrinkage. At any rate, more work is needed to identify a quantitative relation between resistance factors and temperature.

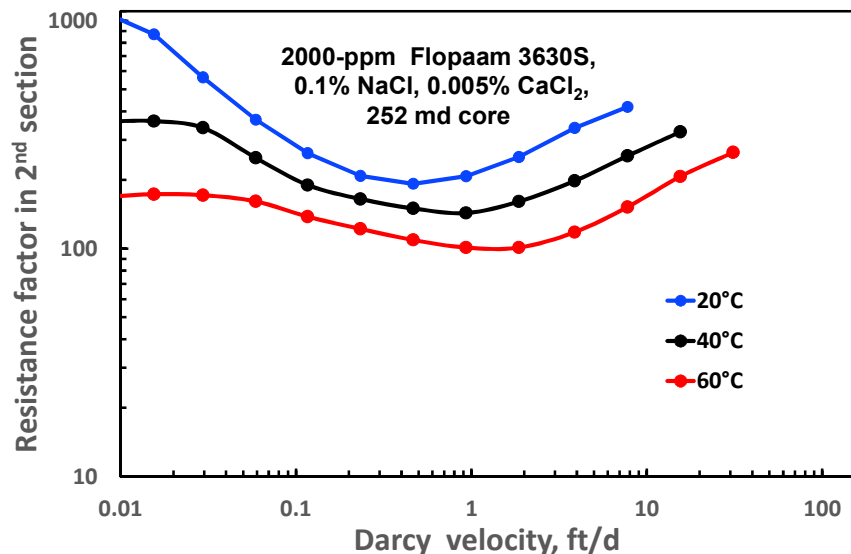


Figure 19—Effect of temperature on 2nd-section resistance factor.

Implications and Relevance to Field Applications.

Of course, the presence of a residual oil saturation normally dramatically reduces the effective permeability to water. That fact means that (other conditions being constant) fracture extension should be much greater if residual oil is present than if it was not (simply because the effective permeability is much lower at S_{or}). Also (other conditions being constant), injection of viscous polymer solutions (including viscoelastic polymer solutions with high viscosity) should lead to greater fracture extension than expected during water injection (simply because polymer solutions are more viscous than water). Beyond these points, the onset of shear thickening and the magnitude of shear thickening can have an important effect on the degree of fracture extension. If the onset velocity for shear thickening moves to a lower velocity as residual oil saturation increases, fracture extension should be greater than if the onset was not affected by the presence of residual oil—because resistance factors are higher above the onset velocity. Also, a greater degree of fracture extension is expected with a large shear-thickening magnitude than a small shear-thickening magnitude.

As mentioned earlier, several previous literature reports, and our current work, revealed that the presence of a residual oil saturation substantially moderates the magnitude of the shear thickening behavior (i.e., the relative increase in magnitude of the resistance factor above the minimum resistance factor, as velocity increases). Thus, above the onset velocity for shear thickening, models/simulations should not assume that data associated with no oil present will be valid if oil is present. Doing so may underestimate injectivity and overestimate fracture extension during injection of synthetic polymers.

Some (Skauge et al. 2018; Masalmeh et al. 2019) suggested that this behavior accounts for polymer injectivity in field applications being surprisingly high, relative to water—implying that open fractures may not be needed to justify relatively high injectivities during HPAM injection into vertical wells. However, further consideration reveals that this implication cannot be valid. In the publications discussed, the resistance factors (at any velocity) were quite high (e.g., 10 or more). Straight-forward applications of the Darcy equation reveal that resistance factors of this magnitude must force open fractures (whether they be natural, previous hydraulic, or newly created) to justify the observed injectivities for HPAM injection into vertical wells, regardless of the assumed rheology (Seright et al. 2009; Khodaverdian et al. 2010; Manichand et al. 2013; Ma and McClure 2017; Sagyndikov et al. 2022; Shankar and Sharma 2022). In very permeable formations such as those that constitute most large polymer floods (i.e., 500 md or more), these fractures are typically quite short (e.g., <50 ft), so that pressure transients are often too fast to allow them to be seen during normal pressure transient analysis (Manichand et al. 2013; Sagyndikov et al. 2022; Shankar and Sharma 2022). These short fracture lengths can be of considerable value in promoting injectivity and sweep efficiency, as well as reducing polymer mechanical degradation (Seright et al. 2009; Seright 2017; Seright and Wang 2023a). Although we understand the political and regulatory pressures to deny the existence of fractures during EOR projects, we advocate that chemical EOR projects will benefit greatly by realistically assessing the extent and orientation of any fractures that might be present. We hope that the experimental observations during this study will be of benefit in conducting those assessments for polymer floods and other chemical floods.

One can speculate on why (mechanistically) the presence of residual oil moderates the magnitude of the shear thickening. Perhaps, as oil saturation increases, the dominant pathways through the porous media have fewer sharp constrictions and contractions—thus, moderating the elongational flow field. As a second possibility, perhaps the elongational flow field is moderated because the shear rate at the oil-water interface is much less than that at a rock-water interface. As a third possibility, if elastic turbulence contributes to the

shear-thickening effect (Howe et al. 2015), perhaps the pliable nature of oil drops or films moderates elastic turbulence. Of course, additional work is needed to sort through the various mechanistic possibilities.

Our findings in Figure 8 indicate that the $[1-\phi(1-S_{or})]/[k k_{rw} \phi(1-S_{or})]^{0.5}$ shift factor works when correlating the velocity onset of shear thickening with the reduction of permeability associated with an S_{or} , so long as the fluid velocity is less than three times the onset of shear thickening. Since this (or very similar) shift factors have regularly been used to project polymer flood performance, our findings should be comforting news to previous simulators. However, data from other literature reports suggest that the onset velocity for shear thickening is insensitive to the presence of oil (Gumpenberger et al. 2012; Skauge et al. 2018; Masalmeh et al. 2019; Alfazazi et al. 2021). If this finding is accepted, it diminishes the importance of shear thickening in both fracture extension and viscoelastic mobilization of capillary-trapped residual oil—because modeling of these phenomena must incorporate that shear thickening does not materialize until much higher fluid velocities than normally assumed. Consequently, further experiments clarifying which view is correct is important. As mentioned in previous discussion, none of the above authors discussed this issue in their papers. So, it is possible that they felt that the unexpected lack of a shift in the velocity onset was simply due to limitations with their data quality.

Reports by some authors (Gumpenberger et al. 2012; Skauge et al. 2018; Alfazazi et al. 2021) also introduce considerable uncertainty about the magnitude of resistance factors that polymers provide in the presence of residual oil—even at velocities below the onset of shear thickening. We suspect that these uncertainties stem from differences in how resistance factor is defined in the presence of residual oil—so the problem may disappear upon further clarification from these previous authors. However, if the issue persists, it could considerably complicate the assumed resistance factors that modelers must input into their simulations. Consequently, clarification of this point is needed during future work.

The onset velocity for shear thickening was insensitive to salinity between 0.1% and 5% TDS. This finding may contradict assumptions that are input into models based on intuition or expectations from linear-oscillatory rheological measurements. Consequently, assumptions about the impact of salinity should be carefully considered before performing modeling studies if a salinity variation is expected. Mechanistically, it may seem surprising that the onset velocity for shear thickening was insensitive to salinity. The increase in viscosity with decreasing salinity is taken as evidence that the polymer is in a much more expanded state at low salinity than at high salinity (Zaitoun et al. 2012). In such an expanded state (at low salinity), one might expect that disentanglement and elongation of a given polymer molecule would be easier at low salinity than at high salinity—resulting in a shift of the onset of shear thickening to higher velocities as salinity decreases. Perhaps, this does not occur because at low salinity, although the polymer is in a very expanded state, its elongation is inhibited by entangled with a larger number of other polymer molecules (than at high salinity). In contrast, at high salinity, the polymer is much more entangled with itself than with other polymers and the entanglements are tighter—so its elongation is determined more by disentanglement of these compact entanglements. Overall, the insensitivity of the onset velocity for shear thickening (to salinity) may be a coincidental balance between these two effects. More work is needed to understand the observed behavior.

With increased temperature, resistance factors decreased by a greater factor than expected from solvent viscosity behavior. If a model/simulation assumes that resistance factors closely follow the temperature dependence of water viscosity, the assumption may need to be reconsidered. In particular, resistance factors appear to be shifted by a factor greater than predicted by a simple Arrhenius analysis.

Conclusions

1. Consistent with previous literature reports, we found that the presence of residual oil, moderates the magnitude of HPAM shear thickening behavior. However, this observation was not sufficient to rationalize the unexpectedly high injectivities of HPAM solutions (relative to water) usually observed during field polymer floods that use vertical injection wells.
2. Our work confirmed that the $[1-\phi(1-S_{or})]/[k k_{rw} \phi(1-S_{or})]^{0.5}$ shift factor was valid with versus without the presence of residual oil. In contrast, data from other literature reports suggest that this shift factor does not appear to be valid if oil is present—in particular, that the onset velocity for shear thickening appeared insensitive to whether or not oil is present. If accepted, this latter suggestion may contradict and substantially complicate assumptions that have commonly been used by modelers/simulators when projecting polymer flood performance.
3. Contrary to expectations suggested by some previous researchers, the velocity for onset of shear thickening behavior (for 0.1-0.2% HPAM with ~19 million g/mol) was insensitive to salinity between 0.1% and 5% TDS.
4. The magnitude of resistance factors associated with shear thickening decreased with increased temperature by a factor greater than expected from consideration of how water viscosity varies with temperature. This decrease could not be explained by oxidative or mechanical degradation of the polymer.

Nomenclature

ATBS	= poly(acrylamide tertiary butyl sulfonic acid)
HPAM	= partially hydrolyzed polyacrylamide or acrylamide-acrylate copolymer
k	= permeability, darcys [μm^2]
k_{rw}	= relative permeability to water at residual oil saturation, darcys [μm^2]
k_w	= permeability to water at residual oil saturation, darcys [μm^2]

M_w = polymer molecular weight, g/mol [daltons]
 PV = pore volumes of fluid injected
 p = pressure, psi [Pa]
 dp/dl = pressure gradient, psi/ft [Pa/cm]
 Δp = pressure drop or difference, psi [Pa]
 R = universal gas constant, 8.314 J/mol-°K
 S_{or} = residual oil saturation
 S_{wr} = connate water saturation
 T = temperature, °K
TDS = total dissolved solids, wt. %
 u = Darcy velocity, ft/d [cm/s]
 μ = viscosity, cp [mPa s]
 μ_o = original viscosity before injection, cp [mPa s]
 μ_s = solvent viscosity, cp [mPa s]
 ϕ = porosity

References

1. Abdullah, M., Seright, R.S., Machado, M.B., Delshad, M., Sepehrnoori, K. 2023. An Analytical Tool to Predict Fracture Extension and Elastic Desaturation for Polymer Field Projects. Paper SPE 215083 presented at the SPE Annual Technical Conference and Exhibition. San Antonio, Texas. 16-18 October. doi:10.2118/215083-MS.
2. Alfazazi, U., Chacko, T.N., Al-Shalabi, E.W., AlAmeri, W. 2021. Investigation of Oil Presence and Wettability Restoration Effects on Sulfonated Polymer Retention in Carbonates Under Harsh Conditions. Paper presented at the Abu Dhabi International Petroleum Exhibition & Conference, Abu Dhabi, UAE, November 2021. doi: 10.2118/207892-MS.
3. Alzaabi, M.A., Jacobsen, J.G., Masalmeh, S. Sumaiti, A.A., Skauge, A., 2020. Polymer Injectivity Test Design Using Numerical Simulation. *Polymers* 2020, 12, 801. doi: 103390/polym12040801.
4. Azad, M.S., Dalsania, Y., Trivedi, J.J. 2018. Understanding the Flow Behavior of Copolymer and Associative Polymers in Porous Media Using Extensional Viscosity Characterization: Effect of Hydrophobic Association. *Canadian Journal of Chemical Engineering* 96(November 2018) 2498-2508. doi: 10.1002/cjce.23169.
5. Azad, M.S., Trivedi, J.J. 2019. Novel Viscoelastic Model for Predicting the Synthetic Polymer's Viscoelastic Behavior in Porous Media Using Direct Extensional Rheology Measurements. *Fuel* 235 (2019) 218-226. doi: 10.1016/j.fuel.2018.06.030.
6. Azad, M.S., Trivedi, J.J. 2020a. Does Polymer's Viscoelasticity Influence Heavy-Oil Sweep Efficiency and Injectivity at 1 ft/D? *SPE Res Eval & Eng* 23(2): 446-462. doi: 10.2118/193771-PA.
7. Azad, M.S., Trivedi, J.J. 2020b. Quantification of Sor Reduction during Polymer Flooding Using Extensional Capillary Number. *SPE J.* 26(3): 1469-1498. doi: [10.2118/204212-PA](https://doi.org/10.2118/204212-PA).
8. Azad, M.S. 2023. Characterization of Nonlinear Viscoelastic Properties of Enhanced Oil Recovery Polymer Systems Using Steady-Shear Rheometry. *SPE J.* 28(2): 664-682. doi: [10.2118/212824-PA](https://doi.org/10.2118/212824-PA).
9. Briscoe, B., Luckham, P., Zhu, S. 1999. Pressure Influences Upon Shear Thickening of Poly(acrylamide) Solutions. *Rheo Acta* 38: 224-238.
10. Cannella, W.J., Huh, C., Seright, R.S. 1988. Prediction of Xanthan Rheology in Porous Media. Paper presented at the SPE Annual Technical Conference and Exhibition, Houston, Texas, October 1988. doi: [10.2118/18089-MS](https://doi.org/10.2118/18089-MS).
11. Chauveteau, G., Moan, M. 1981. The Onset of Dilatant Behaviour in Non-Inertial Flow of Dilute Polymer Solutions Through Channels of Varying Cross-Sections. *Le Journal de Physique Letters* 42(10) L-201.
12. Delshad, M., Kim, D.H., Magbagbeola, O.A., Huh, C., Pope, G.A., Tarahhom, F. 2008. Mechanistic Interpretation and Utilization of Viscoelastic Behavior of Polymer Solutions for Improved Polymer-Flood Efficiency. Paper presented at the SPE Symposium on Improved Oil Recovery, Tulsa, Oklahoma, USA, April 2008. doi: 10.2118/113620-MS.
13. Durst, F., Hass, R., Interthal, W. 1982. Laminar and Turbulent Flows of Dilute Polymer Solutions: A Physical Model. *Rheol. Acta* 21 572-577.
14. Green, D.W., Willhite, G.P. 2018. Enhanced Oil Recovery, 2nd Edition. Society of Petroleum Engineers Textbook Series: 175.
15. Gumpenberger, T., Deckers, M., Kornberger, M., Clemens, T. 2012. Experiments and Simulation of the Near-Wellbore Dynamics and Displacement Efficiencies of Polymer Injection, Matzen Field, Austria. Paper presented at the Abu Dhabi International Petroleum Conference and Exhibition, Abu Dhabi, UAE, November 2012. doi: 10.2118/161029-MS.
16. Heemskerck, J., Rosmalen, R., Janssen-van, R., Holtslag, R.J., Teeuw, D. 1984. Quantification of Viscoelastic Effects of Polyacrylamide Solutions. Paper presented at the SPE Enhanced Oil Recovery Symposium, Tulsa, Oklahoma, April 1984. doi: 10.2118/12652-MS.
17. Hirasaki, G.J., Pope, G.A. 1974. Analysis of Factors Influencing Mobility and Adsorption in the Flow of Polymer Solution Through Porous Media. *SPE J.* 14(4): 337-346. doi: [10.2118/4026-PA](https://doi.org/10.2118/4026-PA).

18. Howe, A.M., Clarke, A., Giernalczyk, D. 2015. Flow of Concentrated Viscoelastic Polymer Solutions in Porous Media: Effect of Mw and Concentration on Elastic Turbulence Onset in Various Geometries. *Soft Matter* 2015, 11, 6419-6431. doi: 10.1039/s5sm01042.
19. Hwang, J., Zheng, S., Sharma, M., Chiotoroiu, M.M., Clemens, T. 2022. Use of Horizontal Injectors for Improving Injectivity and Conformance in Polymer Floods. Paper presented at the SPE Improved Oil Recovery Conference, Virtual, April 2022. doi: 10.2118/209373-MS.
20. Jennings, R.R., Rogers, J.H., West, T.J. 1971. Factors Influencing Mobility Control by Polymer Solutions. *J Pet Technology* **23**(3): 391-401. doi: 10.2118/2867-PA.
21. Jouenne, S., Heurteux, G. 2020. Correlation of Mobility Reduction of HPAM Solutions at High Velocity in Porous Medium with Ex-Situ Measurements of Elasticity. *SPE J.* **25** (1): 465–480. doi: 10.2118/198899-PA.
22. Khodaverdian, M., Sorop, T., Postif, S., an den Hoek, P. 2010. Polymer Flooding in Unconsolidated-Sand Formations: Fracturing and Geomechanical Considerations. *SPE Prod Oper* **25**(2): 211–222. 2010. doi: 10.2118/121840-PA.
23. Li, Z., Espinoza, D.N., Balhoff, M.T. 2023. Simulation of Polymer Injection in Granular Media: Implications of Fluid-Driven Fractures, Water Quality, and Undissolved Polymers on Polymer Injectivity. *SPE J.* **28**(1): 289–300. doi: 10.2118/200412-PA.
24. Lohne, A., Nodland, O., Stavland, A., Hiorth, A. 2017. A Model for Non-Newtonian Flow in Porous Media at Different Flow Regimes. *Comput Geosci* 21: 1289-1312. doi: 10.1006/s10596-017-9692-6.
25. Lotfollahi, M., Farajzadeh, R., Delshad, M., Al-Abri, A., Wassing, B.M., Al-Mjeni, R., Awan, K., Bedrikovetsky, P. 2016. Mechanistic Simulation of Polymer Injectivity in Field Tests. *SPE J.* **21**(4): 1178–1191. doi: 10.2118/174665-PA.
26. Ma, Y., McClure, M.W. 2017. The Effect of Polymer Rheology and Induced Fracturing on Injectivity and Pressure-Transient Behavior. *SPE Res Eval Eng* **20**(2): 394–402. 2017. 10.2118/184389-PA.
27. Magbagbeola, O.A. 2008. Quantification of Viscoelastic Behavior of High Molecular Weight Polymers Used for Chemical Enhanced Oil Recovery. UT-Austin, MS Thesis.
28. Masalmeh, S., AlSumaiti, A., Gaillard, N., Daguerre, F., Skauge, T., Skauge, A. 2019. Extending Polymer Flooding Towards High-Temperature and High-Salinity Carbonate Reservoirs. Paper presented at the Abu Dhabi International Petroleum Exhibition & Conference, Abu Dhabi, UAE, November 2019. doi: 10.2118/197647-MS.
29. Masuda, Y., Tang, K., Miyazawa, M., Tanaka, S. 1992. 1D Simulation of Polymer Flooding Including the Viscoelastic Effect of Polymer Solution. *SPE Res Eng* **7**(2): 247–252. doi: [10.2118/19499-PA](https://doi.org/10.2118/19499-PA).
30. Rock, A., Hincapie, R.E., Tahir, M., Langanke, N., Ganzer, L. 2020. On the Role of Polymer Viscoelasticity in Enhanced Oil Recovery: Extensive Laboratory Data and Review. *Polymers*. 2020, 12 (2276). doi: 10.3390/polym12102276.
31. Sagyndikov, M., Seright, R.S., Kudaibergenov, S., and Ogay, E. 2022. Field Demonstration of the Impact of Fractures on HPAM Injectivity, Propagation and Degradation. *SPE J.* **27**(2) 999-1016. doi:10.2118/208611-PA.
32. Seright, R.S, Maerker, J.M., and Holzwarth, G.M. 1981. Mechanical Degradation of Polyacrylamides Induced by Flow Through Porous Media. *American Chemical Society Polymer Preprints*, **22**: 30–33.
33. Seright, R.S. 1983. The Effects of Mechanical Degradation and Viscoelastic Behavior on Injectivity of Polyacrylamide Solutions, *SPE J.* **23**(3): 475–85. doi: [10.2118/9297-PA](https://doi.org/10.2118/9297-PA).
34. Seright, R. 1991. Effect of Rheology on Gel Placement. *SPE Res Eng* **6**(2): 212-218; *Transactions AIME* 291. doi: [10.2118/18502-PA](https://doi.org/10.2118/18502-PA).
35. Seright, R., Seheult, M., and Talashek, T. 2009. Injectivity Characteristics of EOR Polymers, *SPE Res Eval & Eng* **12**(5): 783-792. doi: 10.2118/115142-PA.
36. Seright, R., Fan, T., Wavrik, K., and Balaban, R. 2011. New Insights into Polymer Rheology in Porous Media. *SPEJ* **16**(1): 35-42. doi: [10.2118/129200-PA](https://doi.org/10.2118/129200-PA).
37. Seright, R.S. 2017. How Much Polymer Should Be Injected during a Polymer Flood? Review of Previous and Current Practices. *SPE J.* **22**(1): 1-18. doi: 10.2118/179543-PA.
38. Seright, R.S., Wavrik, K.E., Zhang, G. AlSofi, A.M. 2021. Stability and Behavior in Carbonate Cores for New EOR Polymers at Elevated Temperatures in Hard Saline Brines. *SPE Res. Eval. Eng.* **24**(1) 1-18. 2021. doi: 10.2118/200324-PA.
39. Seright, R.S., Wang, D. 2023a. Polymer Flooding: Current Status and Future Directions. *Petroleum Science* **20**(2023): 910-921. doi: 10.1016/j.petsci.2023.02.002.
40. Seright, R.S. Wang, D. 2023b. Impact of Salinity, Hardness, Lithology, and ATBS Content on HPAM Polymer Retention for the Milne Point Polymer Flood. Paper SPE 212946 presented at the SPE Western Regional Meeting, Anchorage, Alaska. 22-25 May. doi:10.2118/212946-MS.
41. Skauge, A., Zamani, N., Jacobsen, J.G., Shiran, B.S., Al-Shakry, B., Skauge, T. 2018. Polymer Flow in Porous Media: Relevance to Enhanced Oil Recovery. *Colloids and Interfaces* 2018, **2**(27). doi: 10.3390/colloids2030027.
42. Wang, D., Li, C., Seright, R.S. 2020. Laboratory Evaluation of Polymer Retention in a Heavy Oil Sand for a Polymer Flooding Application on Alaska's North Slope. *SPE J.* **25**(4) 1842-1856. doi:10.2118/200428-PA.
43. Willhite, G.P., Uhl, J.T. 1988. Correlation of the Flow of Flocon 4800 Biopolymer with Polymer Concentration and Rock Properties in Berea Sandstone, Water-Soluble Polymers for Petroleum Recovery, G.A. Stahl and D.N. Schulz (eds.) Plenum Press, New York City (1988) 101-119.
44. Zaitoun, A., Makakou, P., Blin, N., Al-Maamari, R.S., Al-Hashmi, A.R., Abdel-Goad, M. Al-Sharji, H.H. 2012. Shear Stability of EOR Polymers. *SPE J.* **17**(2): 335–339. doi: 10.2118/141113-PA.

45. Zeynalli, M., Al-Shalabi, E.W., AlAmeri, W. 2023. An Extended Unified Viscoelastic Model for Predicting Polymer Apparent Viscosity at Different Shear Rates. *SPE Res Eval & Eng* **26**(1): 99–121. doi: [10.2118/206010-PA](https://doi.org/10.2118/206010-PA).

SI Metric Conversion Factors

cp x 1.0*	E-03	= Pa·s
ft x 3.048*	E-01	= m
in. x 2.54*	E+00	= cm
mD x 9.869 233	E-04	= μm^2
psi x 6.894 757	E+00	= kPa

* Conversion is exact.